Tailoring Mechanical Properties of a Multi-Principle-Element Alloy by a Multi-Length-Scale Approach

NATIONAL ENERGY TECHNOLOGY LABORATORY

AASC Advanced Alloys Signature Center

Chang-Yu Hung[1,2], *Milan Heczko*[3], Chenyang Li[4], Dallin J. Barton[5], Paul Jablonski[1], Wei Chen[4], Arun Devaraj[5], Michael J. Mills[3], Martin Detrois[1], Stoichko Antonov[1]

[1] National Energy Technology Laboratory, 1450 Queen Ave. SW, Albany, OR 97321, USA
[2] NETL Support Contractor, 1450 Queen Ave. SW, Albany, OR 97321, USA
[3] The Ohio State University, 2041 College Road, Columbus, OH 43210, USA
[4] University at Buffalo, The State University of New York, Buffalo, NY 14260, USA
[5] Pacific Northwest National Laboratory, Richland, WA, USA

Presented at TMS 2025, Las Vegas, NV

March 24, 2025

U.S. DEPARTMENT OF ENERGY

Disclaimer

U.S. DEPARTMENT of ENERGY | NATIONAL ENERGY TECHNOLOGY LABORATORY

TWIP NiCo-based alloys – Age Hardening Response

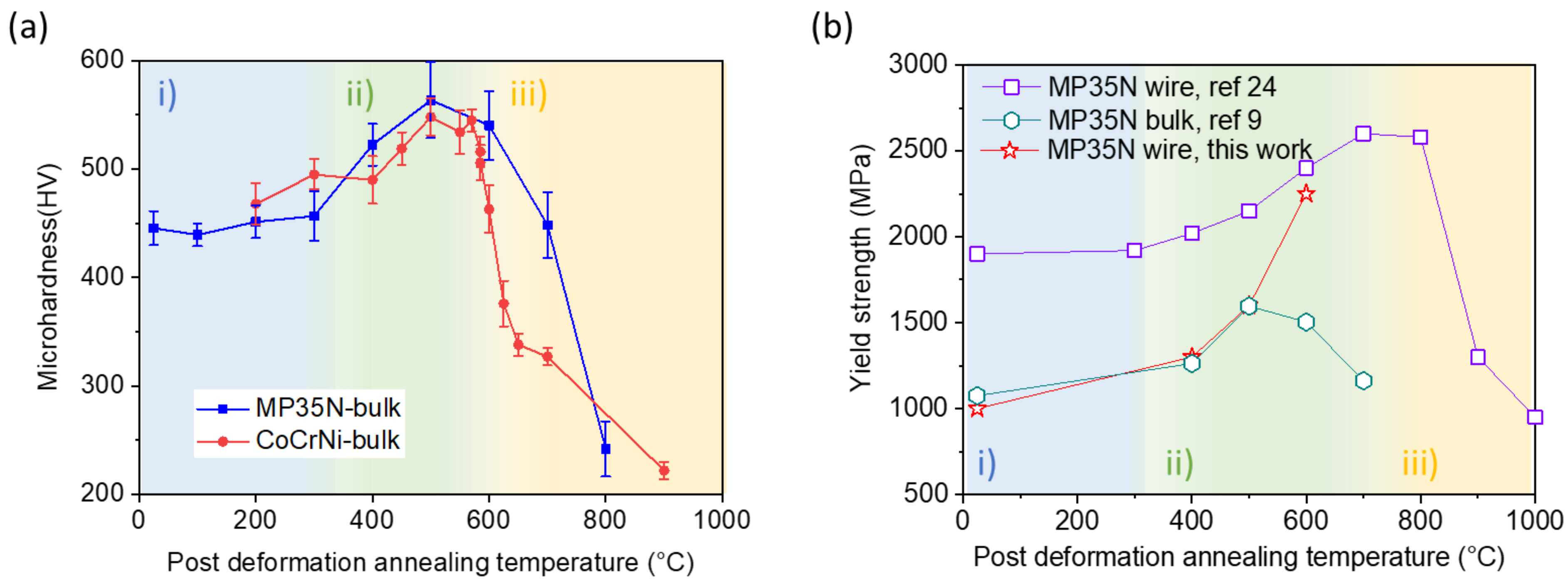

- MP35N (35Ni-35Co-25Cr-10Mo in at%) and similar alloys have exhibited interesting age-hardening behavior for single phase γ alloys
- Good combination of high strength, toughness and fatigue resistance
- Single phase -> age hardening? How can we utilize it to our needs?

Antonov, S., et al. (2020). *Scripta Materialia*, 208.

TWIP NiCo-based alloys – Age Hardening Response

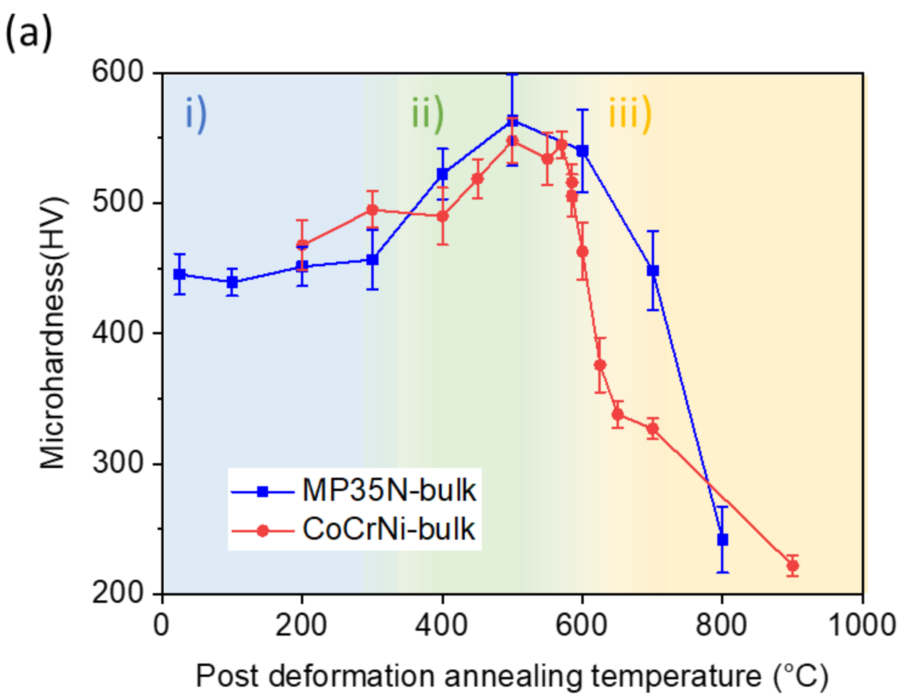

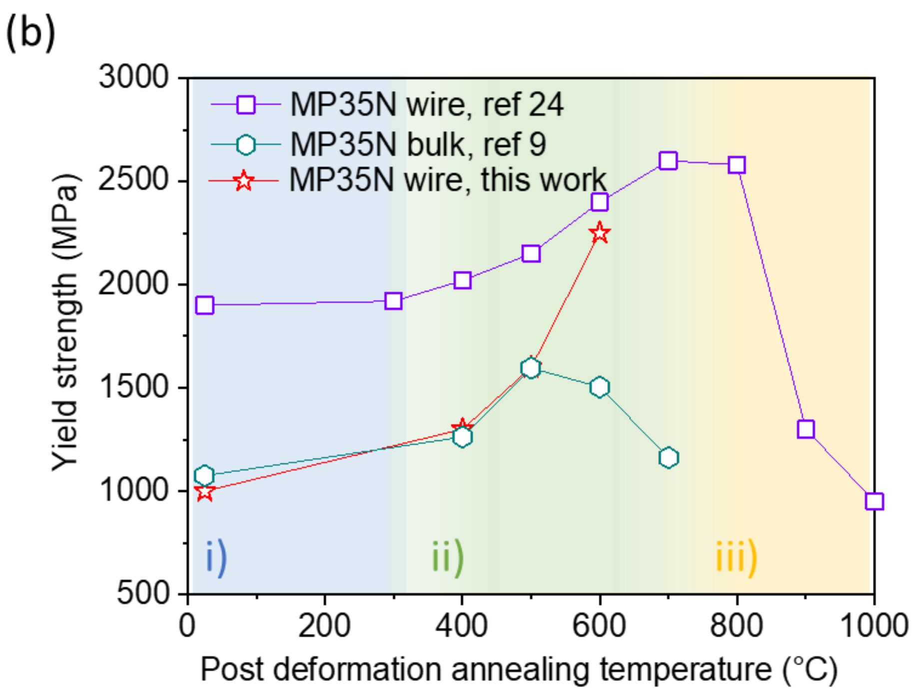

- MP35N (35Ni-35Co-25Cr-10Mo in at%) and similar alloys have exhibited interesting age-hardening behavior for single phase γ alloys
- Good combination of high strength, toughness and fatigue resistance
- Single phase -> age hardening? How can we utilize it to our needs?

Antonov, S., et al. (2020). *Scripta Materialia*, 208.

Materials and Processing

- VIM Melted 8 kg ingots
- Computationally optimized homogenization
- Upset forging (1150°C)
- Hot rolling (1150°C)

In wt.%
From XRF analysis for major elements, LECO for C and N and calculated from addition to the melt for B, plus minor impurities.

Alloys	Ni	Co	Cr	Mo	B
DT-0	100	-	-	-	-
DT-1	35.0	35.0	30.0	-	0.03
DT-2	35.0	35.0	25.0	5	0.03
DT-3	35.0	35.0	20.0	10	0.03

Hung, C., et al. (2025). *Acta Materialia*, 120918.

Starting Microstructure

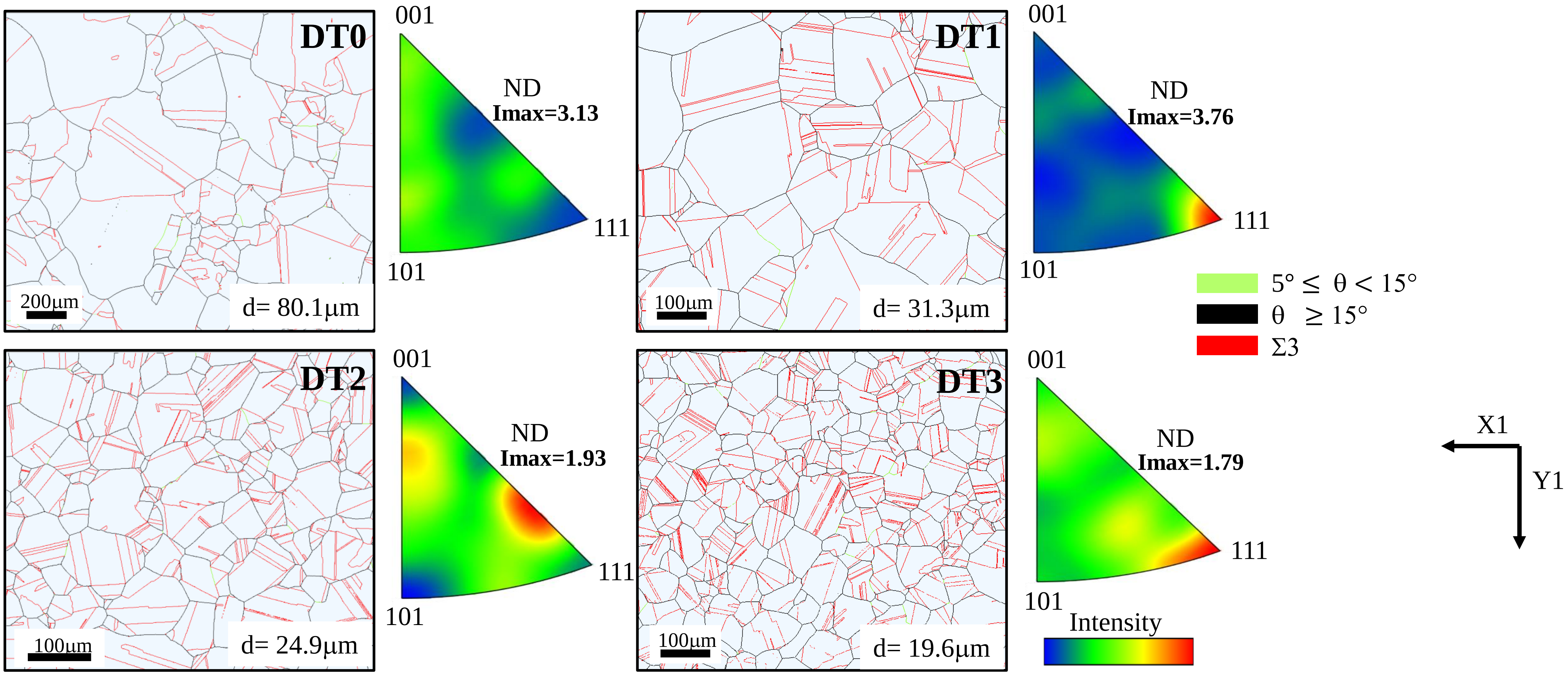

- Mo additions slow down grain growth and lead to smaller grain size

Tensile Properties of Annealed Material

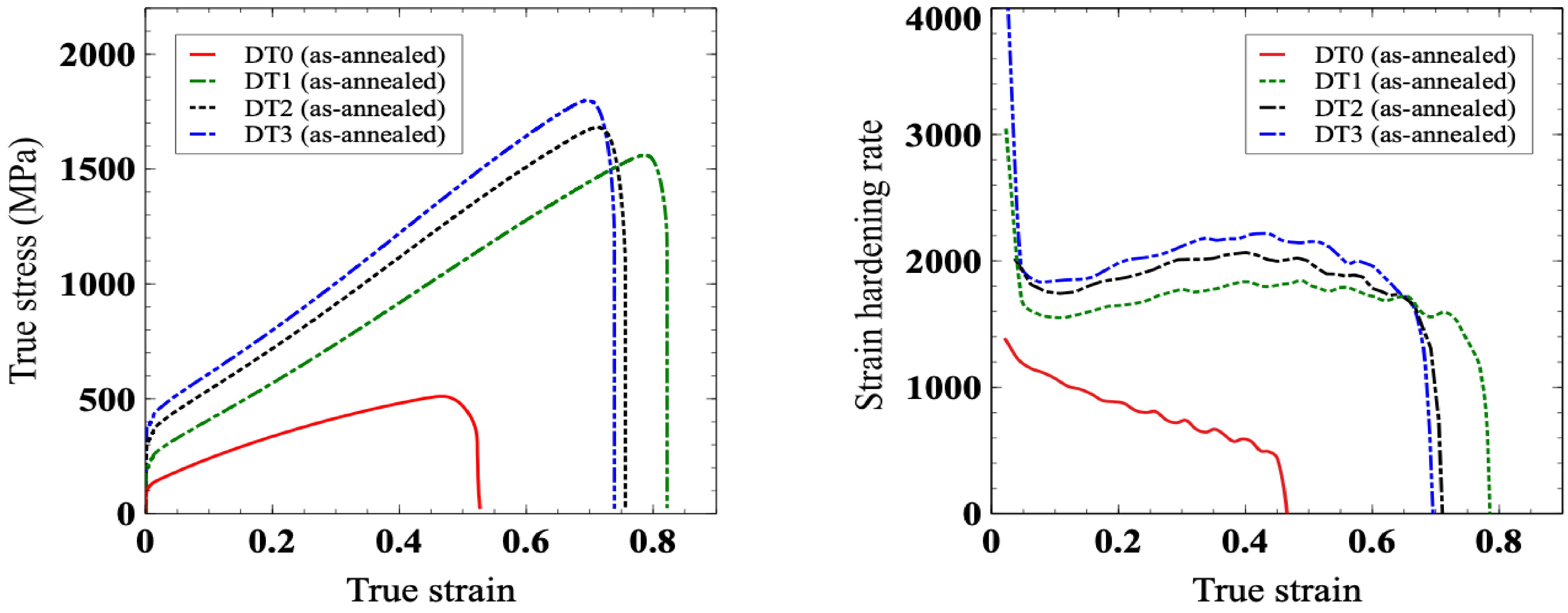

- Low yield strength (~204-376MPa) with ↑ Mo
- Improved ductility vs pure Ni
- Very high strain hardening with steady increase from 0.1 to 0.5 strain compared to decrease in Ni

Effect of Mo on the Back Stress

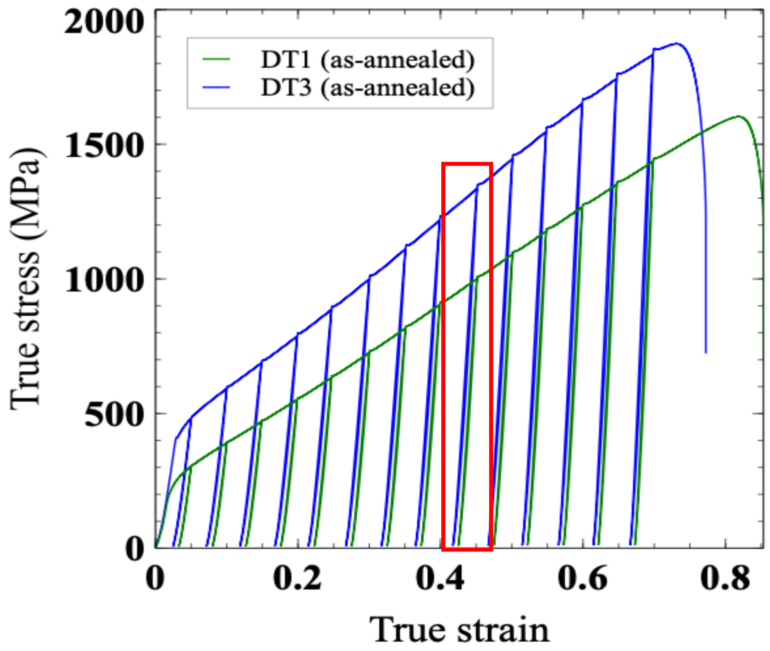

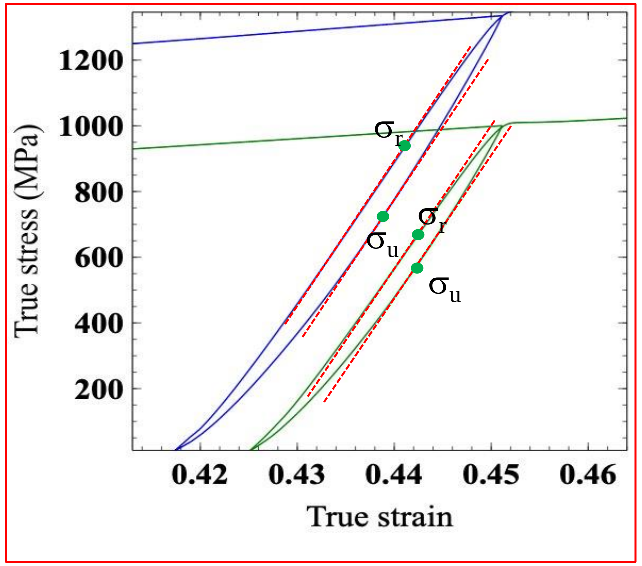

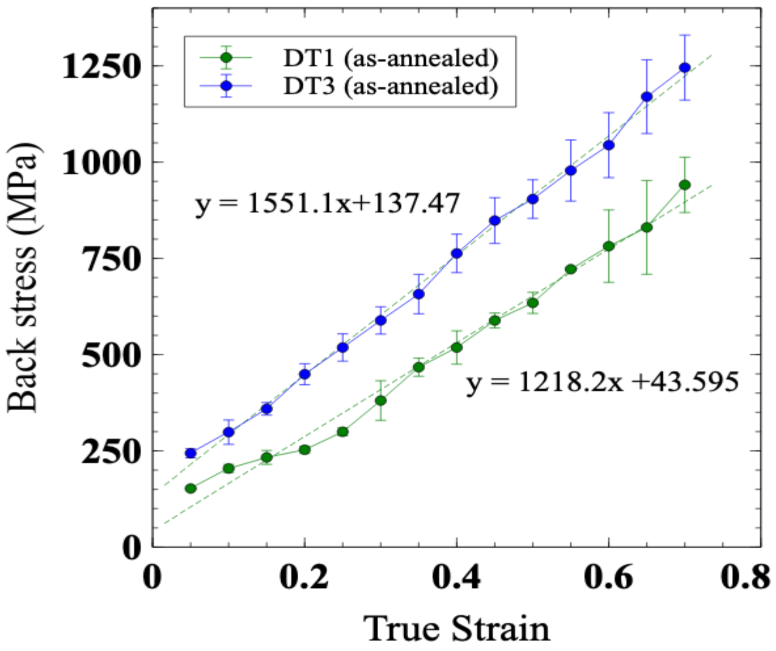

$$\text{Back stress} = \frac{(\sigma_r + \sigma_u)}{2}$$

- Loading-unloading-reloading was conducted to understand local back stresses from pile-up
- Back stress was calculated from hysteresis loop of the curves (3 samples per alloy)
- At 0.7 true strain (prior to necking), the back stress of DT3 is as high as ~1.2 GPa and ~300 MPa higher than that of DT1

Defect Structure of Pre-Strained Alloys

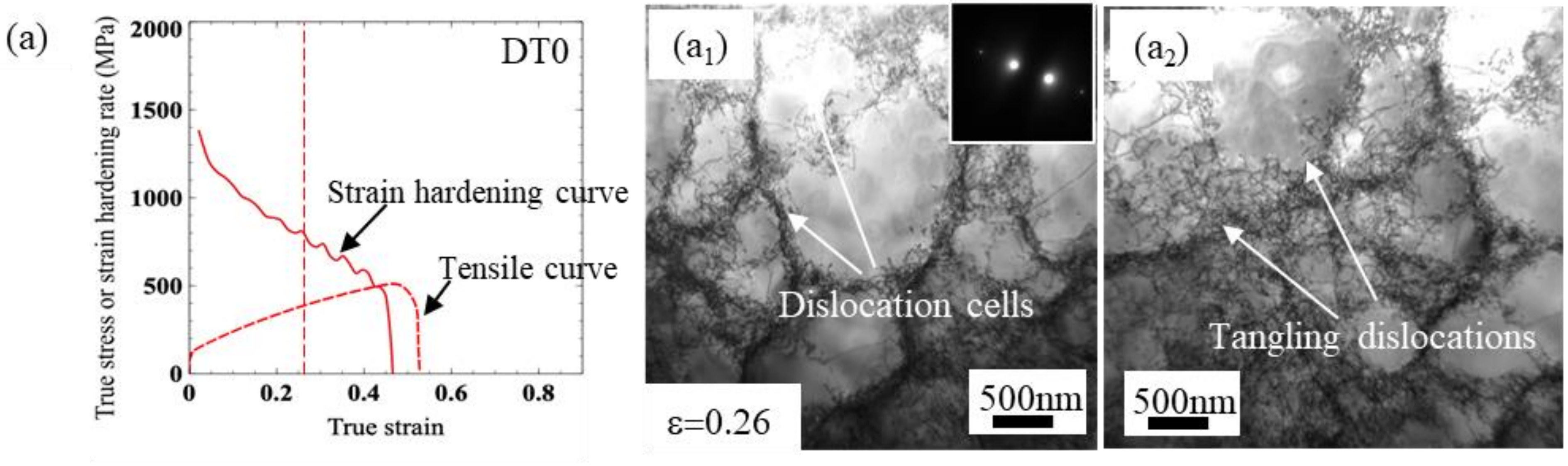

- The primary deformation microstructure for DT0, subjected to tensile interruption at a true strain of 0.26, is heterogeneous dislocations gliding on multiple slip systems
- Result in the formation of dislocation cells, consistent with observations reported for medium-to-high SFE metals

Defect Structure of Pre-Strained Alloys

- The main microstructural features after deformation are stacking faults and nano-twins
- Streaks and extra diffraction spots in SADs correspond to the stacking faults and deformation twins oriented edge-on
- Observed intersections of non-parallel stacking fault systems, indicated by the yellow circles

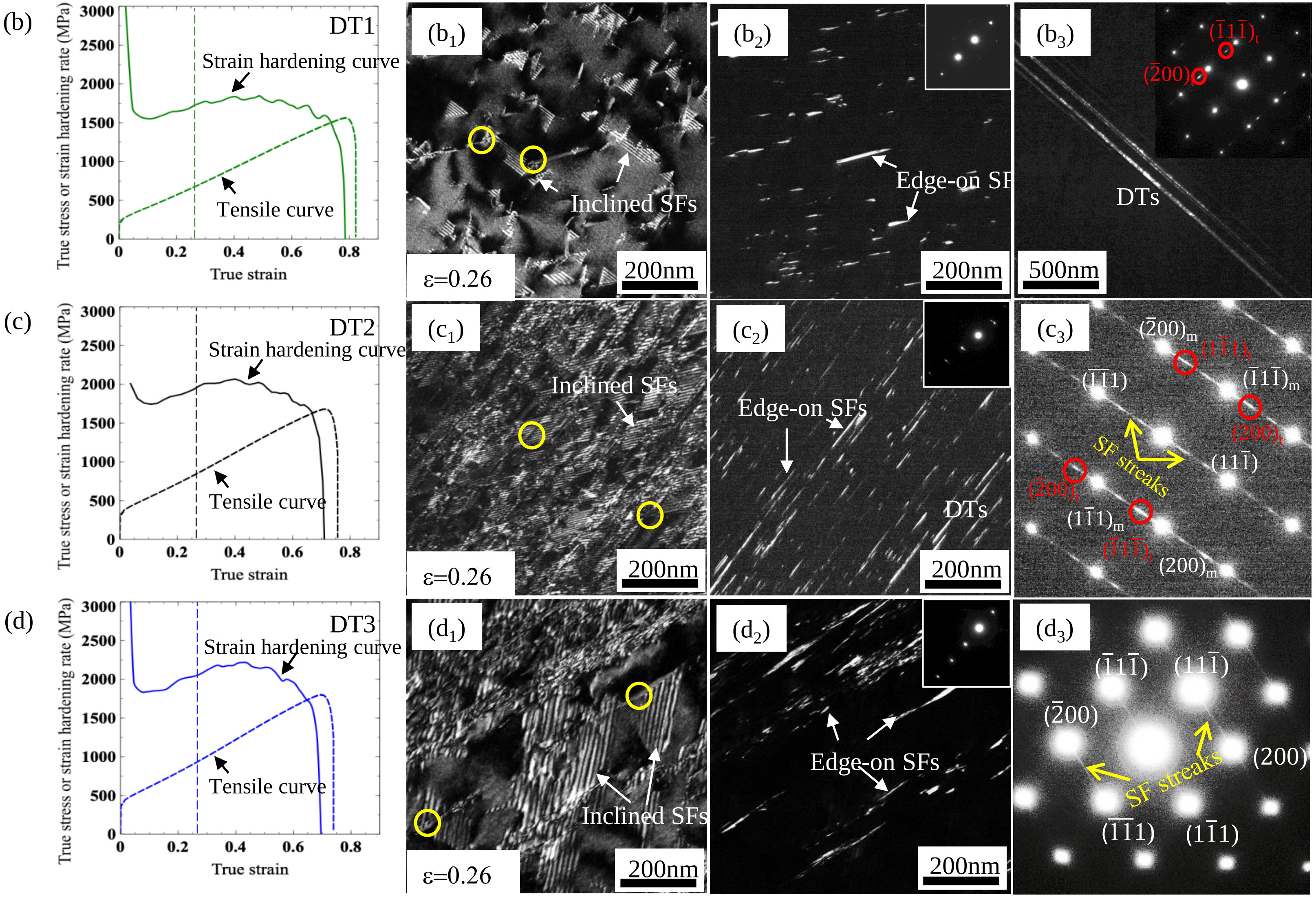

Hung, C., et al. (2025). *Acta Materialia*, 120918.

Heat Treating Pre-Strained Tensile Samples

- Tensile tests interrupted at 0.26 and 0.47 strain to heat treat at 500°C for 1 hr before testing again
- Decrease in strength in Ni vs significant increase in the DT alloys as a function of pre-strain amount
- DTs retain high strain hardening rate
- Can achieve 2.3 GPa in the 10-Mo added DT3 while maintaining a notable fracture elongation of 12%

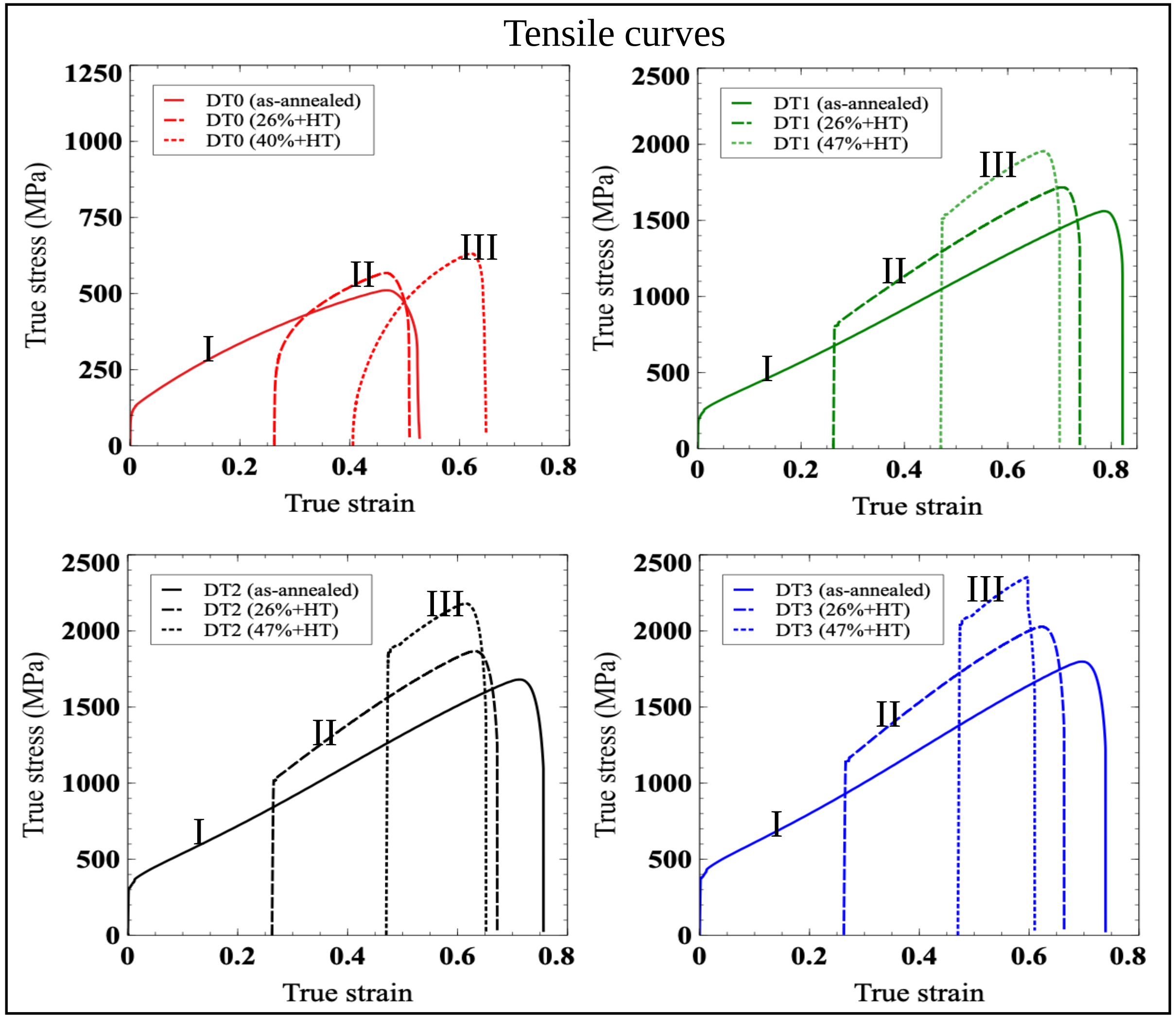

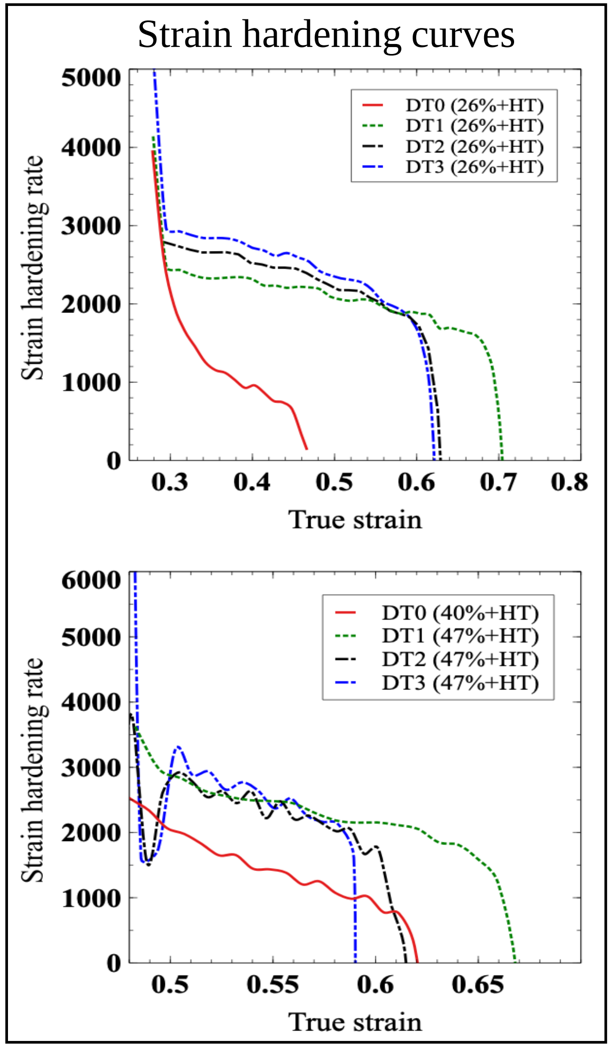

Pre-Strained and Heat-Treated Microstructures

- Weak <111> texture in all samples
- Pure Ni, DT0, exhibits low misorientation grains indicative of recrystallization at 500°C
- The grain misorientation across the entire scanned region of DT1 and DT3 remains high, underscoring that the heat treatment did not significantly annihilate GNDs or causing recrystallization

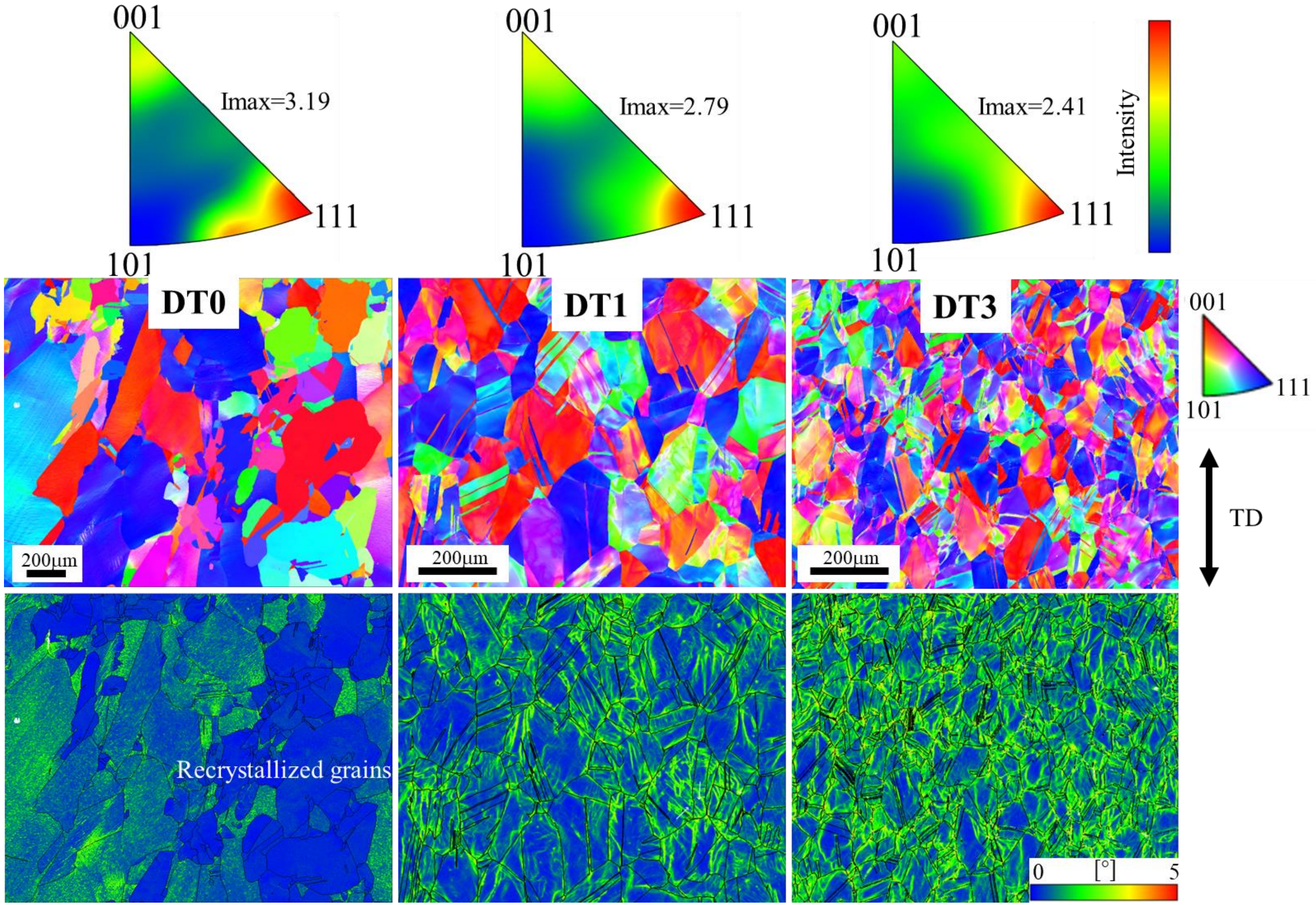

Effect of Pre-Strain + HT on the Back Stress

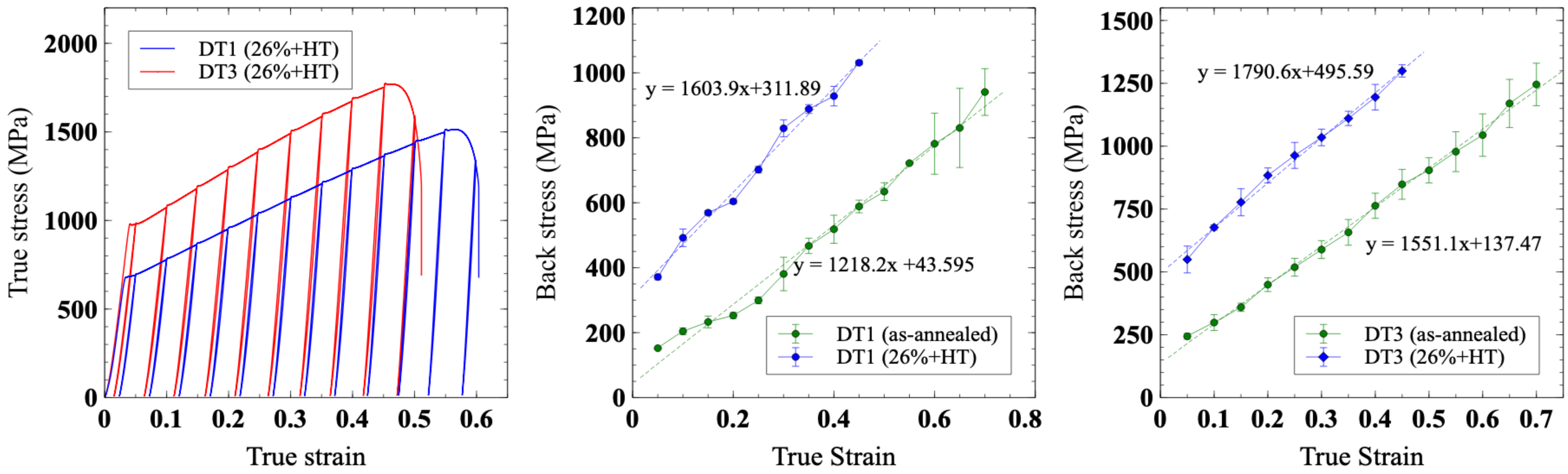

- The loading-unloading-reloading responses remain similar to the as-annealed, but with a higher true stress level due to the strengthening caused by the heat treatment
- Steeper slope of back-stress increment for DT alloys with heat treatment indicates that back-stress was intensified and caused by strong barriers to dislocation motion

Deformation microstructure of pre-strained + HT alloys

- High level of deformation defects remain, showing that the heat treatment does not eliminate the pinned partial dislocations
- Some unlocked SFs expand and terminate at intersection nodes (highlighted by yellow and red circles) wherever they encounter other SFs lying on conjugate slip planes
- The intersection nodes circled in yellow are known for containing Lomer-Cotrell (L-C) locks with sessile dislocations acting as strong barriers to the motion of incoming dislocations

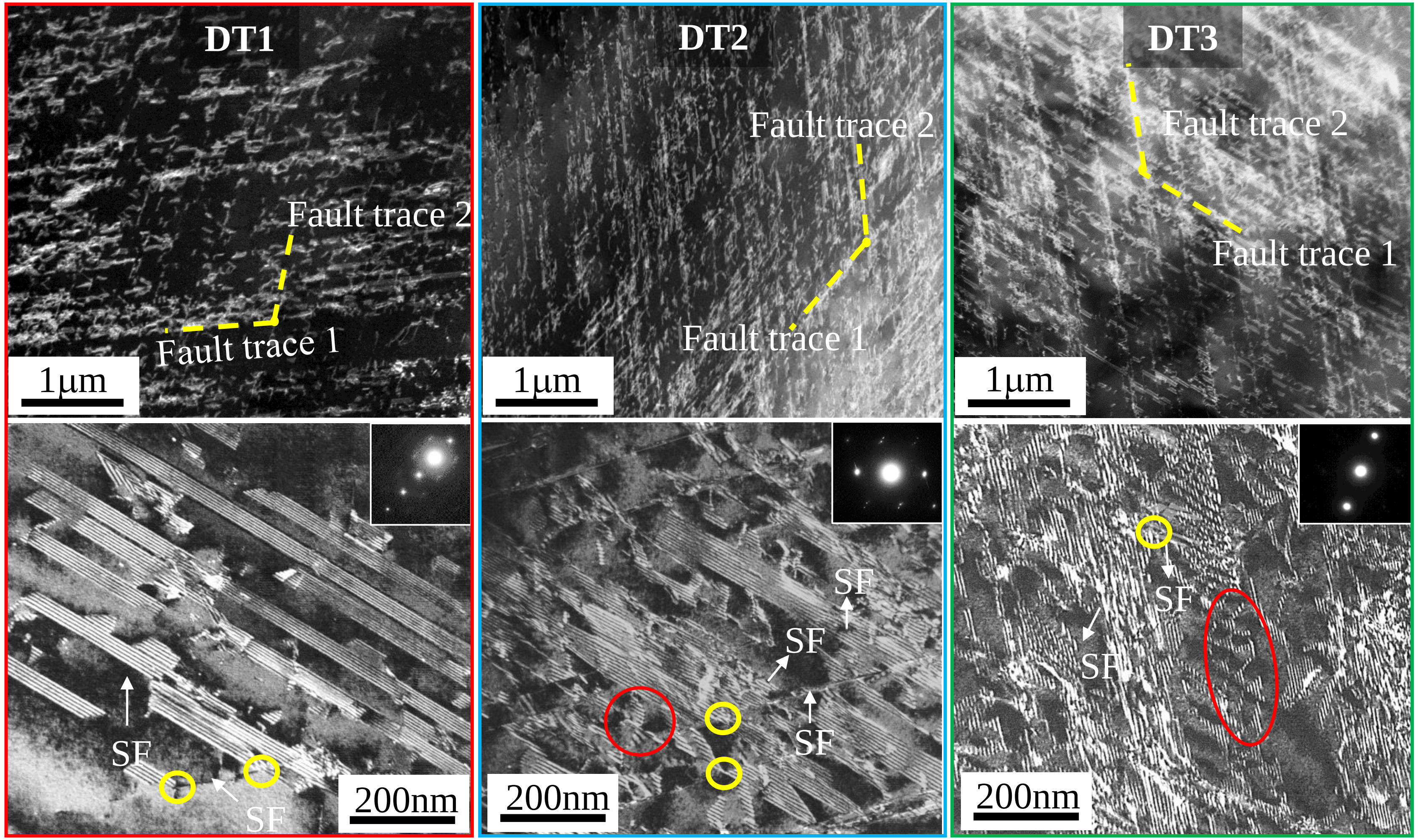

Hung, C., et al. (2025). *Acta Materialia*, 120918.

Sub-structure of Pre-strained + HT alloys

U.S. DEPARTMENT of ENERGY | NATIONAL ENERGY TECHNOLOGY LABORATORY

- (Uneven) Cr Segregation to fault planes was observed at the expense of Co/Ni, but minimal variation in Mo
- A slight Cr depletion was detected adjacent to the fault plane, indicating localized diffusion
- The Cr segregation width appears much thicker than what a structural fault plane would be, indicating that there is likely a gradient of Cr segregation across the fault plane as a result of the strain gradient
- The Cr segregation is expected to increase the SF width and node size due to a local reduction of SFE, however no local structural transformation observed

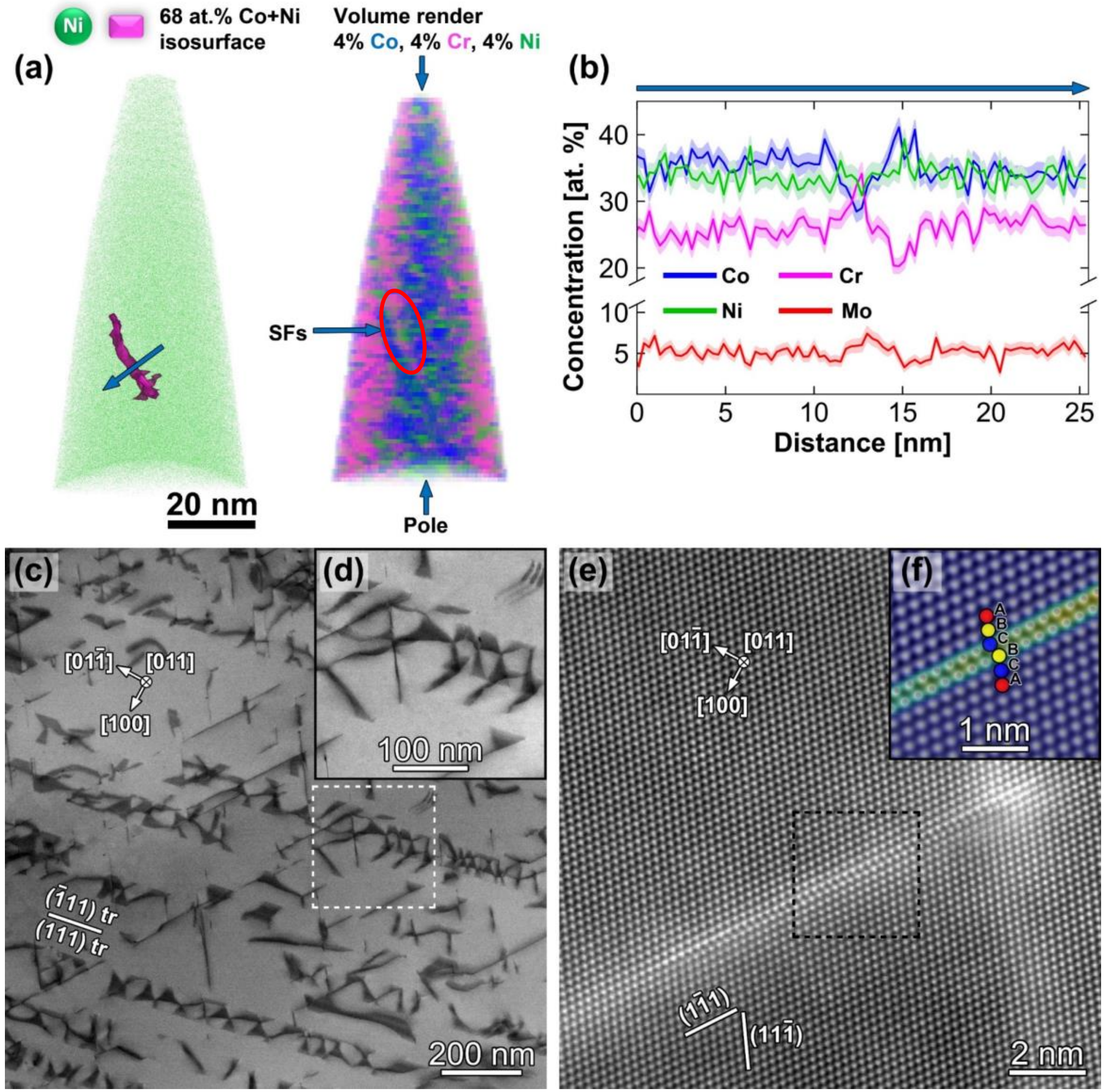

Hung, C., et al. (2025). *Acta Materialia*, 120918.

SFE Considerations due to Cr Segregation

- Compositions around the DT1 and DT2 space show a linear relationship with Cr/Co ratio, decreasing SFE with increasing Cr/Co (segregation conditions)
- Mo addition introduces complexity to the SFE landscape that universally reduces the SFE and enables facile SF expansion and intersection

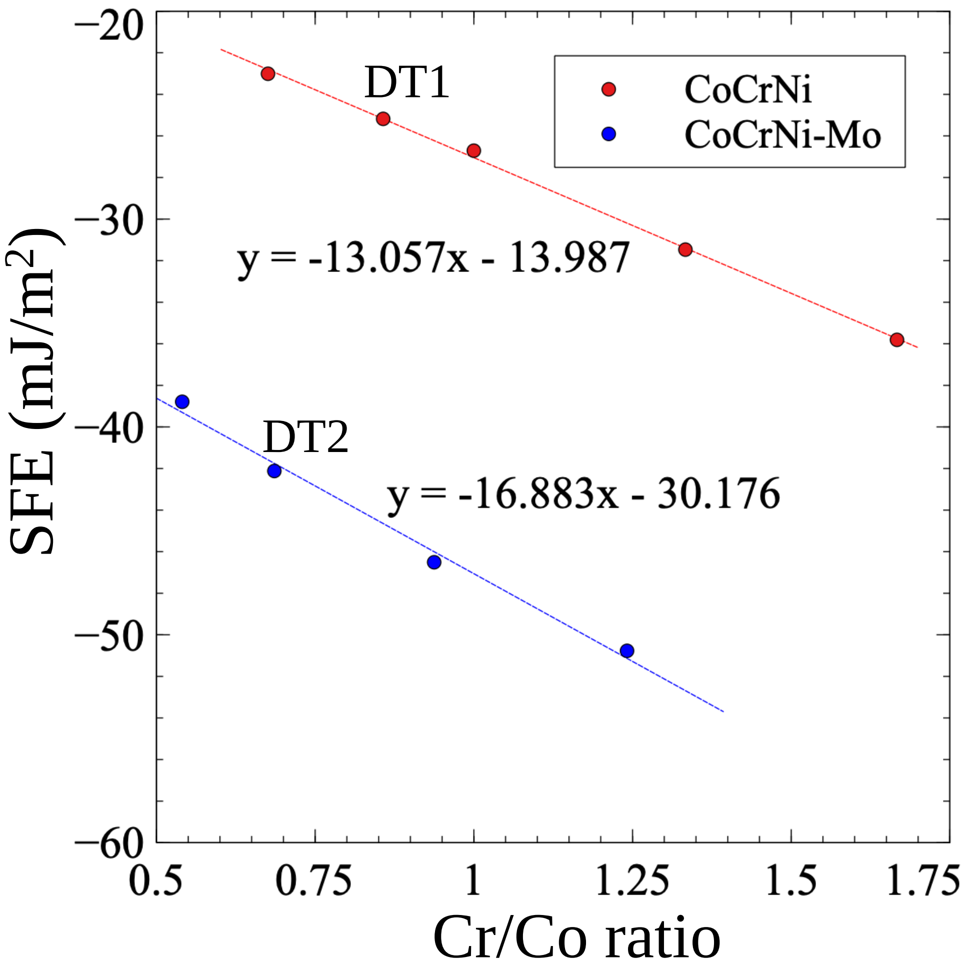

Hung, C., et al. (2025). *Acta Materialia*, 120918.

SF expansion and interaction

- V-shaped SFs configurations are frequently observed in the DT alloys post pre-strain + HT, containing a stair-rod dislocation
- Qi et al. suggest that L-C locks were frequently observed in acute-angle V-shaped configuration while obtuse-angle V-shaped SF configuration usually leads to Hirth locks

1. $a/6[233] = a/2[011]_{perfect} + a/3[100]_{Hirth\ sessile}$
2. $a/3[100]_{Hirth\ sessile}$
3. $a/3[100]_{Hirth\ sessile}$
4. $a/6[2\overline{33}] = a/2\,[0\overline{11}]_{perfect} + a/3\,[100]_{Hirth\ sessile}$

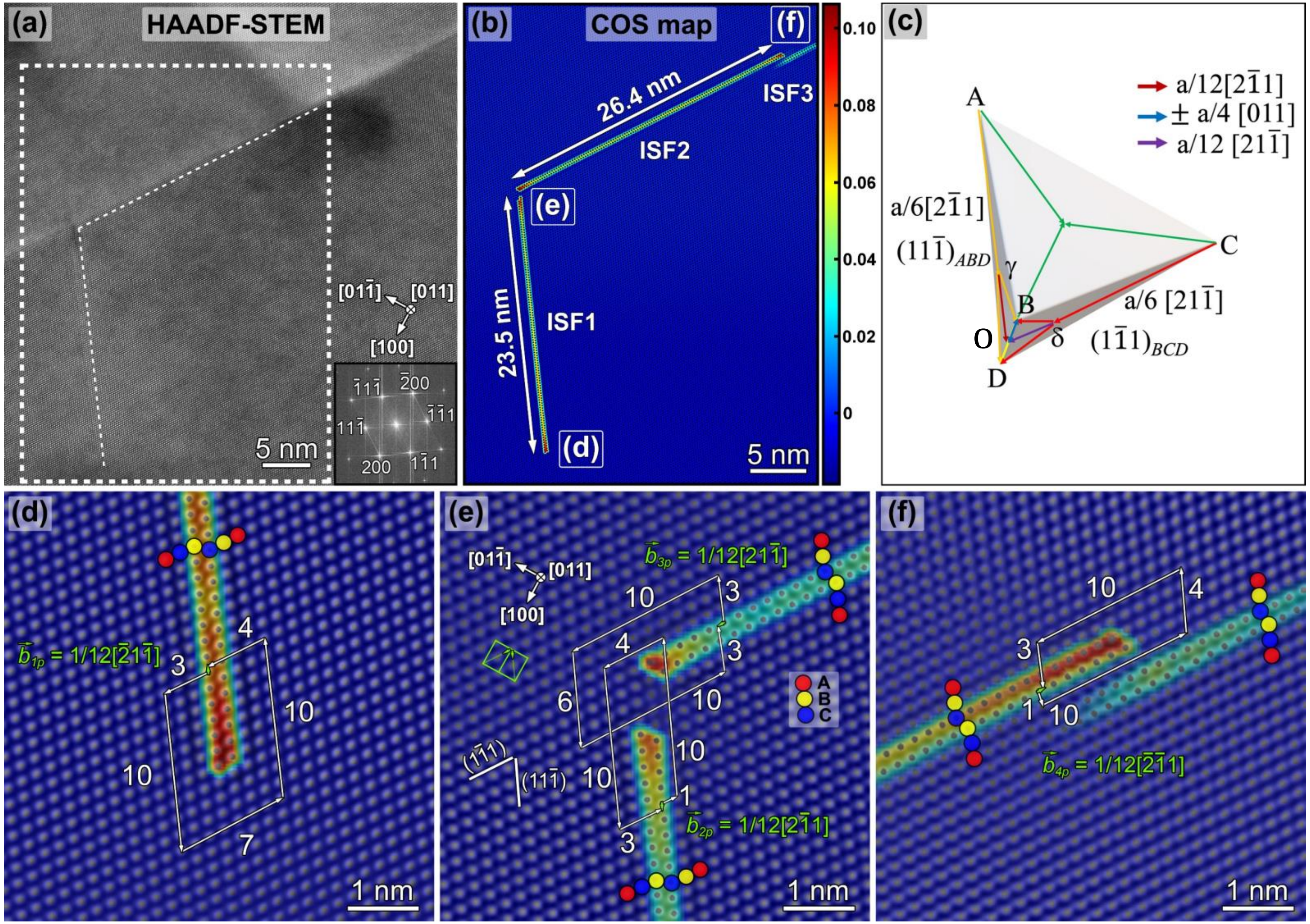

Qi, L., et al. (2020). *Acta Materialia*, 649.

Hung, C., et al. (2025). *Acta Materialia*, 120918.

Effect of Mo and Pre-Strain + HT

- Prior strain followed by a sub-recrystallization-temperature heat treatment extensively promotes a secondary hardening while maintaining an excellent ductility.
- The values of Δσ1 and Δσ2 shows a proportional increase in relation to prior strain level, i.e., the more SFs that formed during prior deformation, the higher the number of preferential Cr segregation sites for further strengthening.
- Level of strengthening also shows a clear relationship to Mo content, as it allows for more SFs to form

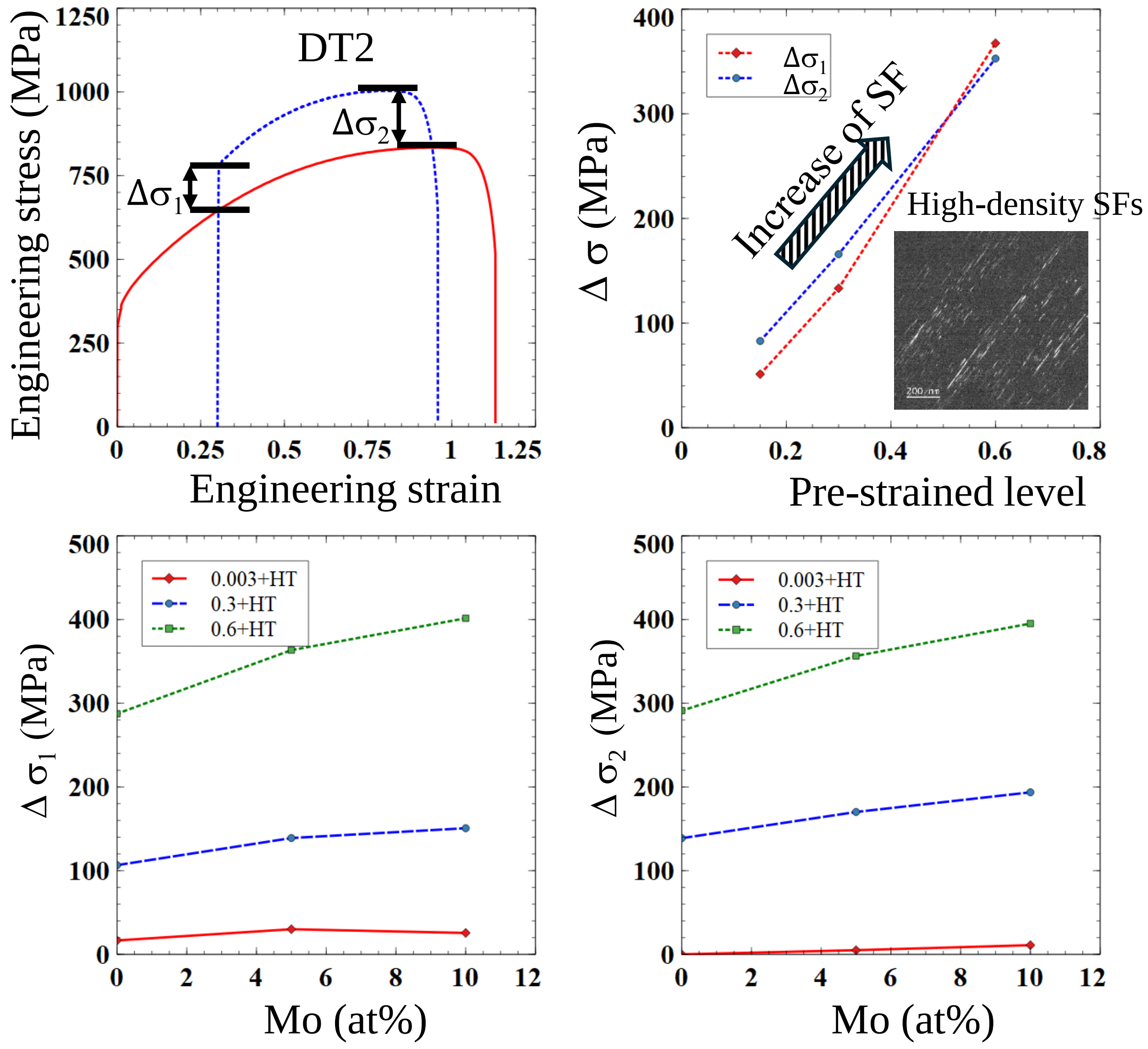

Relationship between Yield Strength and Mo content

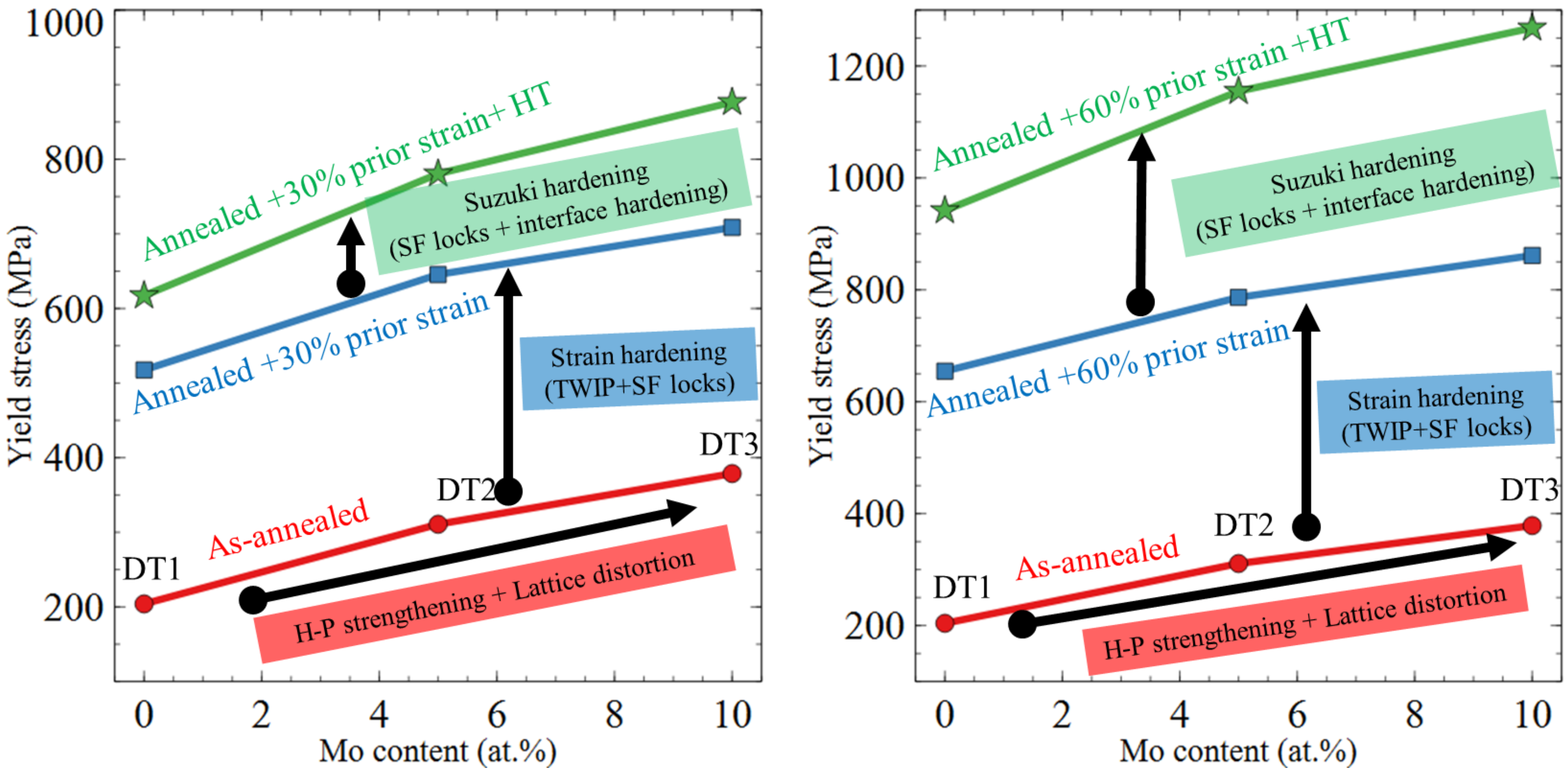

1) Hall-Petch strengthening and lattice distortion in as-annealed DT alloys (red curves)
2) Strain hardening via TWIP effect and SF locks (blue curves)
3) Suzuki segregation strengthening Cr segregation, further SF locks and interface hardening (green curves)

Conclusions

This study presents an alternative strategy for tailoring the mechanical properties of NiCoCr-based MPEAs and related alloys:

- Mo strengthens the material through lattice distortion, Hall-Petch strengthening, and reduction of SFE, which promotes complex stacking fault (SF) interactions that hinder dislocation mobility
- SFs (stacking faults) act as preferential sites for Cr segregation, reducing the stacking fault energy (SFE) and impacting dislocation mobility, with a decrease in SFE as the Cr/Co ratio increases
- The reduced local SFE in SFs allows them to expand and interact with other faulting systems, enhancing strength and strain hardening through V-shaped configurations of L-C and Hirth locks

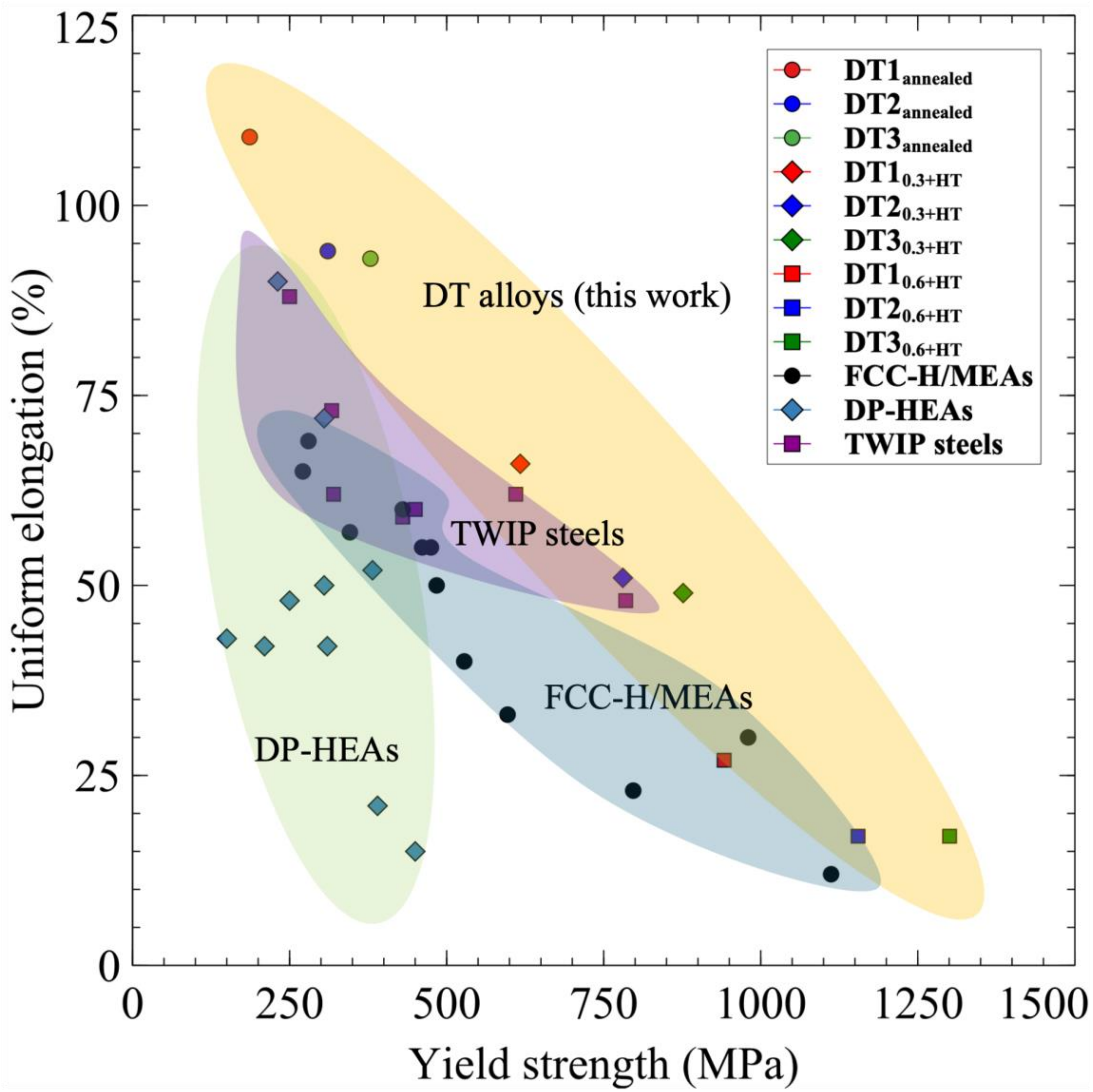

Hung, C., et al. (2025). *Acta Materialia*, 120918.

Acknowledgments

This work was performed in support of the US Department of Energy's Fossil Energy and Carbon Management Office's Advanced Energy Materials Research Program and executed through the National Energy Technology Laboratory Research & Innovation Center (Advanced Energy Materials MYRP-1025034). The authors would like to thank C. McKaig and J. Willis for assistance in melting, R.E. Chinn and C. McKaig for chemistry analysis, and Christopher D. Powell for tensile tests. MJM and MH acknowledge financial support from the National Science Foundation under GOALI: / DMREF NSF #2323717. The multi-scale electron microscopy-based characterization was partially performed at the Center for Electron Microscopy and Analysis (CEMAS) at The Ohio State University. Atom probe tomography from PNNL was supported by the U.S. Department of Energy, Office of Science, Basic Energy Sciences, Materials Sciences and Engineering Division as a part of the Early Career Research program (FWP # 76052). The APT was conducted using facilities at Environmental Molecular Sciences Laboratory (EMSL), which is a DOE national user facility funded by Biological and Environmental Research Program located at Pacific Northwest National Laboratory. W. C. and C.L. acknowledges the support by the National Science Foundation under Grant No DMR-2415119.

VISIT US AT: **www.NETL.DOE.gov**

@NETL_DOE

@NETL_DOE

@NationalEnergyTechnologyLaboratory

U.S. DEPARTMENT OF ENERGY

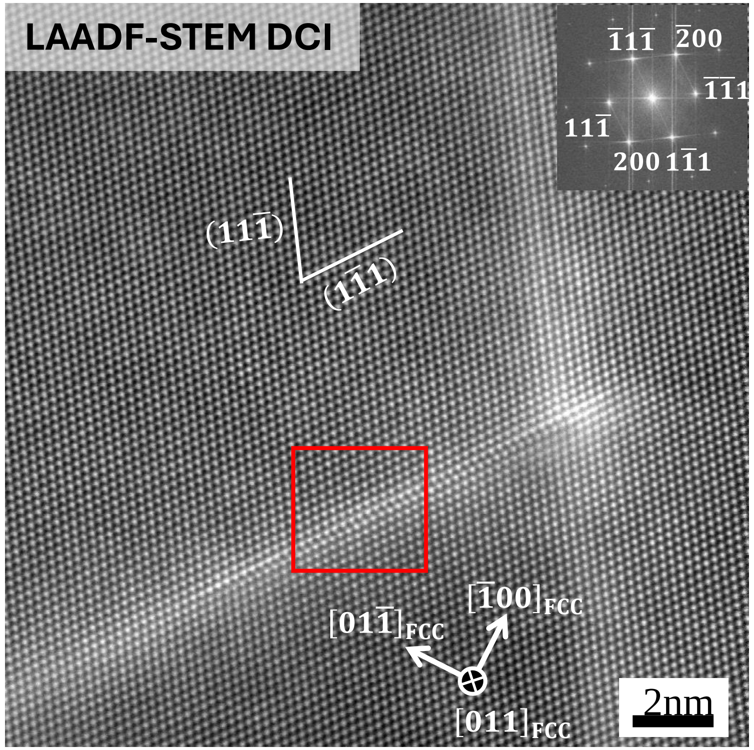
LAADF-STEM DCI
$\bar{1}1\bar{1}$ $\bar{2}00$
$\bar{1}11$
$11\bar{1}$
200 $1\bar{1}1$
$(11\bar{1})$
$(1\bar{1}1)$
$[01\bar{1}]_{FCC}$
$[\bar{1}00]_{FCC}$
$[011]_{FCC}$
2nm

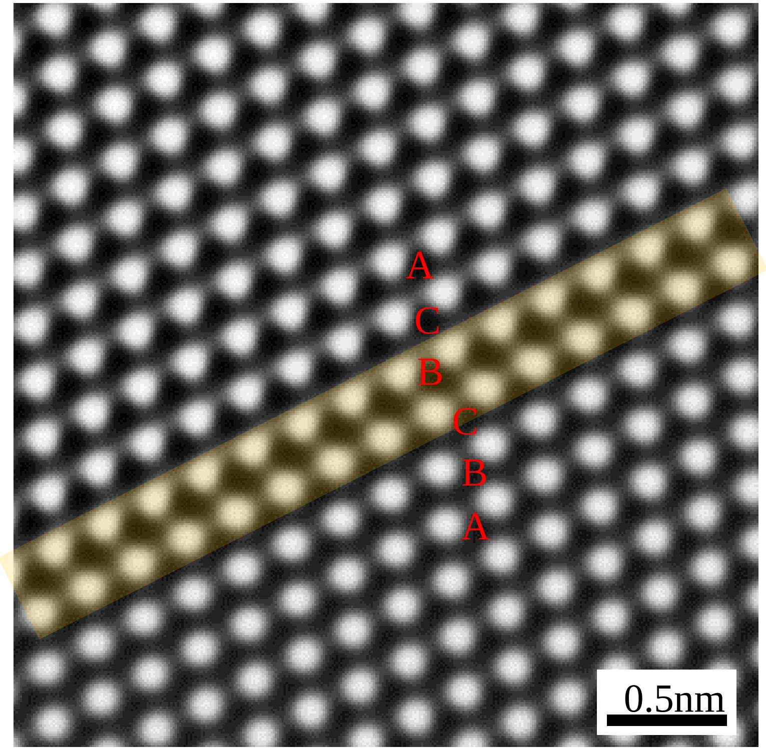
A
C
B
C
B
A
0.5nm

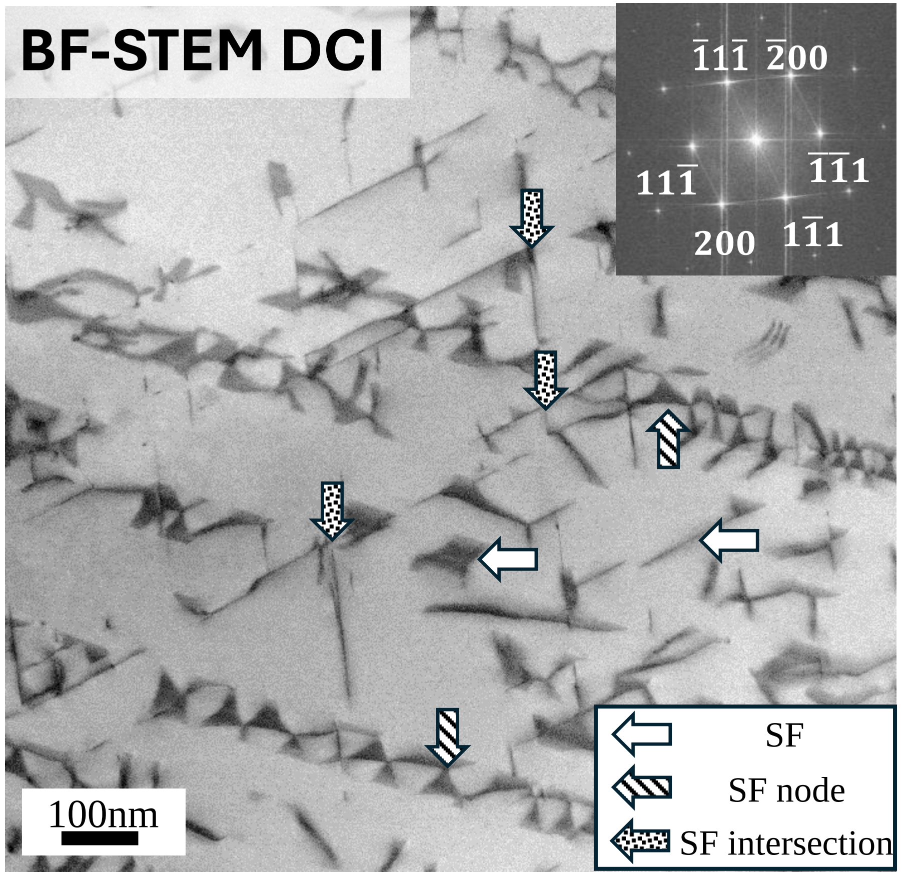
BF-STEM DCI
$\bar{1}1\bar{1}$ $\bar{2}00$
$11\bar{1}$
$\bar{1}11$
200 $1\bar{1}1$
100nm
SF
SF node
SF intersection